Understanding Palladium Hydrogenation Catalysts: When the Nature of the Reactive Molecule Controls the Nature of the Catalyst Active Phase**

Detre Teschner, Zsolt Révay, János Borsodi, Michael Hävecker, Axel Knop-Gericke, Robert Schlögl, David Milroy, S. David Jackson, Daniel Torres, and Philippe Sautet*

Dedicated to the Catalysis Society of Japan on the occasion of the 50th anniversary

Catalytic hydrogenations are one of the most important processes in the chemical industry and selectivity is a timely issue. The presence of triple-bonded compounds in the alkene stream is undesirable in both chemical and polymer-grade propylene and ethylene, as they poison the polymerization catalysts.[1] Starting with a mixture of alkynes and alkenes, palladium-based catalysts are known to be capable of selectively hydrogenating triple bonds, leaving the olefinic function intact. The presence of carbonaceous deposits was assumed to play a key role, influencing the performance of the catalyst.[2] Although the origin of this behavior is unknown, very recently a relation between selectivity and subsurface chemistry has been established, showing that the population, by either hydrogen or carbon, of subsurface sites of palladium governs selective alkyne hydrogenation.[3] Hydrogen in the subsurface is known to play a crucial role in hydrogenating surface species effectively.[4,5]

Herein, we extend our previous studies addressing the fundamental differences of carbon–carbon double or triple bond hydrogenation over Pd. The present results provide solid evidence that differences in the hydrogenation of alkynes and alkenes results from the markedly different state of the near-surface regions. We show that the formation of the Pd/C surface phase is directly related to the nature of the reactive molecule, being a general pattern for alkyne hydrogenation and absent for alkenes. We show in addition that the presence of this Pd/C phase affects the surface chemistry by decreasing the amount of activated subsurface hydrogen compared to the more selective surface hydrogen, hence controlling the state of the Pd catalyst surface under reaction conditions.

To investigate the nature of the active Pd surface, we have studied, by in situ X-ray Photoelectron Spectroscopy (XPS), the near-surface region of palladium under various hydrogenation conditions for various reacting alkynes and alkenes. Under reduced pressure conditions (1 mbar), alkynes are hydrogenated to alkenes while alkenes are transformed to alkanes, just as at more realistic, atmospheric conditions. Figure 1 summarizes the state of palladium under such hydrogenation conditions. The palladium 3d core level was found to be the best indicator of the near-surface state.[3] While the metallic bulk peak is observed at 335 eV, a strong new component (filled peak in Figure 1) appears when alkynes are hydrogenated selectively. This peak, at 335.6 eV, is characteristic of the carbon-modified, Pd/C surface phase. Note that adsorbates give rise to a surface state at similar energy (adsorbate-induced surface core-level shift). However, at the applied 720 eV excitation energy, the contribution from this state should be less than 25% of the whole peak intensity.

Clearly, all the investigated alkynes induce the formation of a Pd/C phase,[3] since the higher binding energy component dominates the spectra. The only difference seems to be in the amount of carbon dissolved in the Pd lattice: for lower chain alkynes more carbon is dissolved in Pd, thickening the Pd/C phase. In contrast, the hydrogenation of alkenes generates a much weaker signal at the higher binding energy side of bulk Pd. According to our fitting procedure, this peak corresponds to roughly one third of the whole signal intensity, which indicates that some carbon is indeed dissolved in the upper part of the metal lattice. However, we attribute the lack of a clearly distinguishable 335.6 eV component to the absence of Pd/C. These results show the widely different nature of the surface under alkyne or alkene feed.

Since palladium is used in industry to hydrogenate alkynes from a mixed alkyne/alkene feed, we have investigated the temporal evolution of the surface using time-resolved in situ XPS, when co-dosing propyne to a propene/H_2 feed. As

[*] Dr. D. Teschner, J. Borsodi, Dr. M. Hävecker, Dr. A. Knop-Gericke, Prof. Dr. R. Schlögl
Fritz-Haber-Institut der Max-Planck-Gesellschaft
Faradayweg 4-6, 14195 Berlin (Germany)
E-mail: teschner@fhi-berlin.mpg.de

Dr. Z. Révay, J. Borsodi
Institute of Isotopes, Hungarian Academy of Sciences, Budapest (Hungary)

Dr. D. Milroy, Prof. Dr. S. D. Jackson
WestCHEM, Department of Chemistry, University of Glasgow (UK)

Dr. D. Torres, Dr. P. Sautet
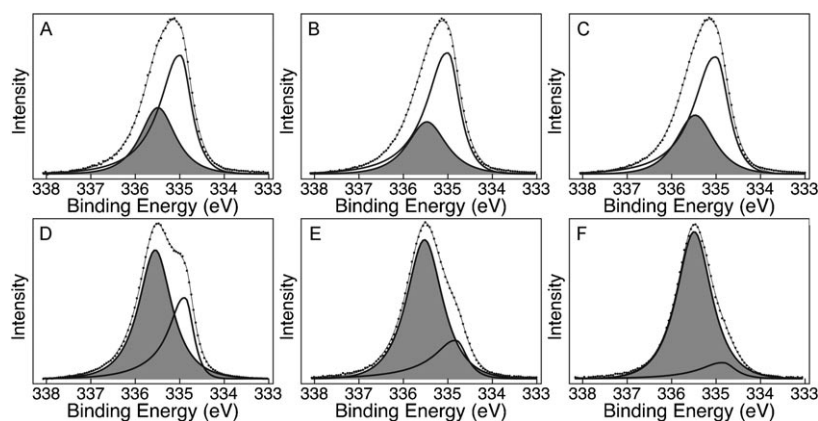Laboratoire de Chimie, Université de Lyon, CNRS (France)

Figure 1. Comparison of in situ Pd $3d_{5/2}$ spectra of Pd foil under alkene and alkyne hydrogenation at 1 mbar (H_2/C_xH_y: 9/1) and 343–353 K. A: 1-pentene; B: propene; C: ethylene; D: 1-pentyne; E: propyne; F: acetylene.

components was inverted, with Pd/C reaching two thirds of the whole signal intensity. The detected temporal profile indicates that the carbon uptake can be divided into two processes: an initial fast step and a second slower step. Since carbon energetically prefers to occupy the first subsurface octahedral sites, we assign the fast step to the occupation of these sites. The very first propyne (alkyne) molecules chemisorbing on Pd undergo fragmentation and the fragments, likely individual carbon atoms, penetrate the surface. Since the second step of Pd/C phase formation is much slower, the build up of additional mixed Pd/C layers should be energetically less favorable. The calculated[6] growth rate of the Pd/C layer is approximately 7 Å h^{-1}, which is equivalent to a diffusion coefficient of carbon (D_c) of approximately 10^{-22} m^2 s, in good agreement with the results of Yokoyama et al.[7] (10^{-23} m^2 s) extrapolated to our temperature.

expected from the previous results, the Pd 3d core level was dominated by the bulk component in the propene + H_2 feed (see Supporting Information, Figure S1). It was however strongly attenuated in the first few minutes after propyne was introduced, and the proportion of the higher binding-energy component slowly increased further in the mixed feed (Figure 2A). After 30 minutes, the ratio of the two Pd
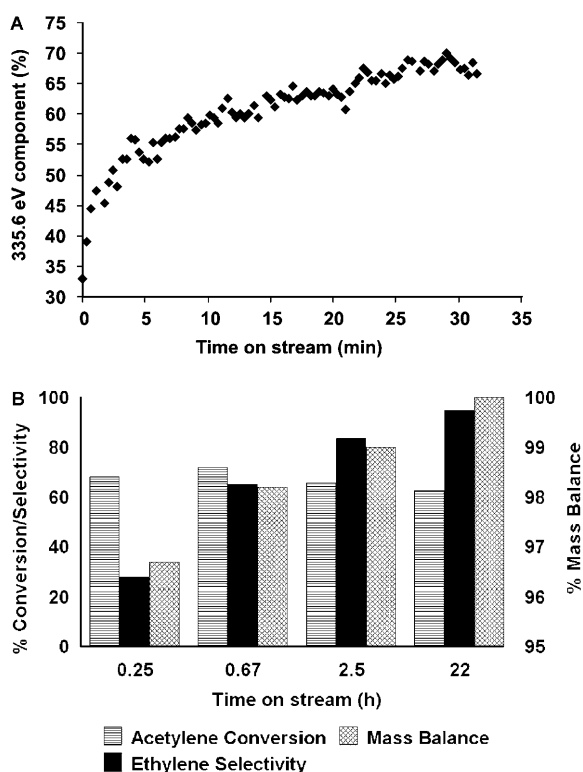
Similar behavior in carbon uptake is also seen over a Pd catalyst under industrially relevant conditions. Figure 2B shows the conversion and selectivity obtained from acetylene hydrogenation. Over the fresh catalyst there is poor alkene selectivity but with time this selectivity increases from 27% to 95%. Over the same period the mass balance increases from 96.5 to 100% showing that as carbon is deposited the selectivity increases. Note that there is little change in activity.

To hydrogenate a given chemical functionality, the catalyst clearly needs hydrogen. For palladium, its propensity to form subsurface- or bulk-dissolved hydrogen (e.g. β-hydride) makes the assignment of the active hydrogen nontrivial. Both, experimental and theoretical studies clearly indicated that hydrogen, when emerging from the subsurface/bulk to the surface, could very effectively hydrogenate different adsorbates.[4,5] If subsurface hydrogen plays an important role in our processes, the occupation of the first subsurface layer with carbon would be critical in the hydrogenation path. To be able to measure and quantify hydrogen dissolved in palladium we have developed prompt gamma activation analysis (PGAA)[8] as an in situ technique.[9] In the PGAA process, the nuclei of chemical elements in the investigated specimen capture neutrons and, during the de-excitation, they emit characteristic prompt gamma photons, which can be detected using an appropriate spectrometer. Hydrogen has a medium neutron-capture cross-section, but gives a strong signal in the gamma spectrum, thus hydrogen atoms dissolved in palladium can be analyzed by PGAA with high sensitivity.

Table 1 compares the hydrogen content of palladium black during 1-pentyne and 1-pentene hydrogenation. When fresh samples are introduced into flowing hydrogen, the hydrogen content matched perfectly the values from the Pd/H phase diagram.[10] Thereafter the H/Pd ratio decreased significantly when selective hydrogenation of 1-pentyne was carried out using a feed ratio (H_2/C_5H_8) of 2.5. The hydrogen content in pure hydrogen of the sample after 1-pentyne hydrogenation (Table 1, H_2 (3rd)) was slightly higher than

Figure 2. A: Temporal evolution of the proportion of the higher binding energy Pd $3d_{5/2}$ component at approximately 335.6 eV after adding 0.1 mbar propyne in the feed of 0.9 mbar H_2 and 0.1 mbar propene according to time-resolved in situ XPS. T: 343 K. B: Change in selectivity of acetylene hydrogenation at 20 bar and 323 K. Catalyst Pd/alumina, Gas Hourly Space Velocity (GHSV): 5000, hydrogen:ethylene:acetylene ratio, 25:25:1.

Table 1: Conversion, product selectivities and atomic H/Pd ratios during in situ PGAA experiments.[a]

Experiments	Conversion [%]	Products [%]	H/Pd
H$_2$[b] (1st)	–	–	0.75
1-pentyne (1st)	21	97.7 1-pentene	0.27
		2.3 pentane	
H$_2$[b] (2nd)	–	–	0.77
1-pentyne (2nd)	44	98.1 1-pentene	0.01
		1.9 pentane	
H$_2$ (3rd)	–	–	0.88
1-pentene (3rd)	99.8	98.6 pentane	0.77
		1.4 2-pentenes	

[a] Sample: 7 mg Pd black; in flowing hydrogen, under 1-pentyne or 1-pentene hydrogenation (after H$_2$ pretreatment); at 1 bar and room temperature. Gas flow during hydrogenation: 4 mL min^{-1} H$_2$ and 1.6 mL min^{-1} C$_5$H$_x$. 1-pentyne hydrogenation was repeated. [b] Fresh Pd black sample.

with fresh sample, suggesting that the surface incorporates carbonaceous deposits containing additional hydrogen. After 1-pentene hydrogenation, the hydrogen content of the sample was even higher than with the equivalent alkyne. This difference can be related to the XPS data (see below).

To achieve an atomistic understanding for the formation of the Pd/C phase, we first addressed the incorporation of C into the Pd substrate. We performed self-consistent density functional theory (DFT) calculations using the VASP code[11] and a periodic Pd(111) model surface.[*] The results of our calculations are shown in Figure 3 (top panels). We determined the average binding energy of carbon (E_b^C) as a function of total C coverage (Θ_C) with different distributions of C between surface, subsurface, and second interlayer. After exploring all possible adsorption site combinations, the most stable situation is shown.

The initial stages in the formation of the Pd/C phase involve the incorporation of carbon from the surface to the first interlayer. Independently of Θ_C, structures involving C atoms adsorbed only in the subsurface are energetically favored (Figure 3, top left panel) with respect to structures involving C adatoms on the surface or on both the surface and subsurface. The most stable conformation corresponds to a $\sqrt{3} \times \sqrt{3}$ distribution of C in the first interlayer.[12] Regarding the C distribution between the first and second interlayer, the situation changes. Placing the C atoms in the second interlayer is roughly as favorable as placing them in the first. For coverage higher than approximately 0.3 monolayer (ML), distribution of the C atoms on both first and second interlayer is energetically more favored than the population of a single interlayer, creating the thermodynamic driving force for the growth of the Pd/C phase. We considered C incorporation into deeper interlayers and, as a general rule, we detected a significant weakening of the average C binding when an increasing number of interlayers were populated; hence this will limit deeper extension of the Pd/C phase.

[*] Note, the Pd(111) surface was used as a model aiming only to extract the main phenomena for C penetration and Pd/C phase formation. Hence DFT was used to qualitatively (and not quantitatively) describe the experiments.
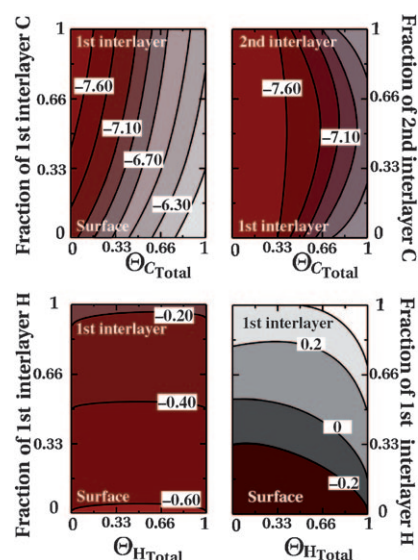

Figure 3. Top: Contour maps showing the average binding energy (color coded, in eV) of carbon as a function of total C coverage (*X* axis) and the distribution of carbon atoms between interlayers (*Y* axis) using a Pd(111) substrate. C atoms are distributed between surface and 1st interlayer sites (left) or between 1st and 2nd interlayer (right). Bottom: Contour maps showing the average binding energy (colour coded, in eV) of hydrogen as a function of total H coverage (*X* axis) on Pd(111) (left) or on the model Pd/C phase (right). H atoms are distributed between surface and 1st interlayer sites.

To describe the XPS experiments herein, at constant pressure and temperature, the appropriate thermodynamic potential to consider is the Gibbs free surface energy $\gamma(T,P)$. This scheme has been successfully applied to various systems,[13] and we will use it to determine the thermodynamically stable composition of the surface in equilibrium with a reactive atmosphere, described by acetylene and hydrogen partial pressures ($p_{C_2H_2}$ and p_{H_2} respectively) at a fixed temperature T. Assuming that thermodynamic equilibrium applies, the environment then acts as a C adatoms reservoir, as it can give or take C atoms from the decomposition or formation of carbon-containing molecules (H atoms concertedly being evolved as H$_2$ to the gas phase). The calculated free surface energy plot as a function of the chemical potential of C (μ_C) is shown in Figure 4. For low values of μ_C, molecule decomposition and C deposition onto the surface is not favored. Only once the μ_C has reached the critical value of -8.8 eV (μ_C^{Crit}), does the carbon deposition start.

When acetylene and hydrogen are dosed onto the catalyst surface, reaction starts and μ_C varies within certain well-defined boundaries. While the upper boundary (μ_C^{Max}) is given by the chemical potential of carbon in the acetylene molecule, the lower boundary is given by the chemical potential of carbon in ethylene, at the given H$_2$ pressure. The formation of the Pd/C phase will be thermodynamically favored under reaction conditions only when μ_C is above the critical equilibrium μ_C^{Crit} value for the migration of carbon to the subsurface. From Figure 4 it is clearly the case for acetylene hydrogenation, but not for ethylene hydrogenation. The stability of this phase for acetylene is dependent on the H$_2$
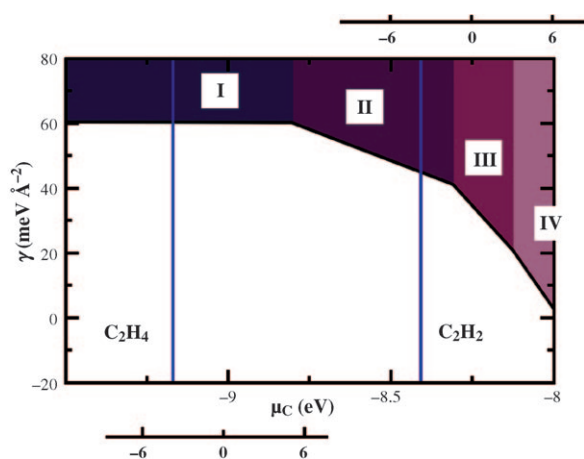
Figure 4. Surface free energy γ (meVÅ^{-2}) of the most stable Pd/C structures as a function of carbon chemical potential μ_C. Structure **I** is the pure Pd(111) surface, **II** has a C content of 1/3 ML in the first interlayer, **III** a C content of 2/3 ML distributed among first and second interlayers, and **IV** a C content of 1 ML distributed in the first three interlayers. Vertical blue lines indicate the μ_C value for the dissociation of acetylene (right line) and ethylene (left line) into C and H$_2$, at pressure conditions employed in XPS (10^{-4}, and 10^{-3} atm for $p_{C_2H_x}$ and p_{H_2}). μ_C is displayed in a logarithmic pressure scale at a fixed temperature of 400 K. Acetylene and ethylene pressures with respect to p_0 (1 atm) are, respectively, shown in the bottom and top X axes.

pressure, because the effective chemical potential of carbon from the molecular reservoir depends on H$_2$ pressure. At high H$_2$ pressure, formation of the phase becomes thermodynamically inhibited.

The difference ($\Delta\gamma^f$) between the surface free energy of the most stable structure and that of the Pd(111) surface, for the μ_C associated to the reactant, can be considered as a descriptor of the thermodynamic driving force for the Pd/C phase formation. For the hydrogenation of acetylene, at typical pressure conditions during in situ XPS (10^{-4} and 10^{-3} atm for $p_{C_2H_2}$ and p_{H_2}), and at 400 K, the formation of the Pd/C phase resulting from the decomposition of acetylene is thermodynamically favored, with $\Delta\gamma^f \approx -25$ meV Å^{-2}. In contrast, the formation of the phase in the presence of ethene is disfavored, with positive $\Delta\gamma^f$. To get more insight into the relation of the Pd/C phase formation with respect to the nature of the reacting molecule we calculated $\Delta\gamma^f$ for a set of reactive molecules of the type HC≡CX, with X = CH$_3$, H, F, Cl (see Supporting Information, Figure S2). The formation of the Pd/C phase is favored for lower-chain alkyne hydrogenation or when electronegative species are attached to the triple bond, qualitatively explaining the thicker Pd/C phase obtained experimentally when going from 1-pentyne, to propyne, to acetylene.

Finally, the presence of C in the subsurface affects the properties of surface hydrogen. To analyze this influence, we compared the binding energy of H on Pd(111) and on a Pd/C phase model. To match the experiments best, we chose structure **IV** of Figure 4, with the first three interlayers occupied with one third C coverage. The average binding energy of H (E_b^H) as a function of total H coverage (Θ_H) was calculated with respect to the gas phase H$_2$ molecule. On the

clean Pd(111) surface, the binding energy does not strongly depend on the coverage (Figure 3, bottom left panel). H is most stable on the surface, but penetration into the subsurface is more favored than desorption.[14] In contrast, the bonding properties of H are strongly modified for Pd/C (Figure 3, bottom right panel). Adsorption on the surface is weakened and, most importantly, the accumulation of H into the subsurface is thermodynamically disfavored. Thus one role of the Pd/C phase is to hinder the migration of H to the subsurface, hence decreasing the H^{sub}/H^{on} ratio in the sample. The Pd/C phase will, in addition, prevent the migration of bulk H toward the surface. Clearly, DFT is in accord with the PGAA results because, once the β-hydride has been depleted, hydrogen is hindered in replenishing the bulk, and the H/Pd ratio will be low. Hence, alkynes are hydrogenated selectively by surface hydrogen, since hydrogen cannot emerge from the bulk, if it is present at all. On the other hand, alkene hydrogenation occurs using subsurface hydrogen, as its concentration is high and no energetic barrier is built up by a subsurface carbon population.

These data clearly indicate that catalytic palladium materials are highly versatile, and their actual (near-)surface compositions are a strong function of the experimental hydrogenation conditions. Understanding such phenomena will allow the design of heterogeneous catalysts to be tailored to a desired reaction. The present study clearly demonstrates the significance of combining theory and experimentation in bringing understanding to a new level.

Experimental Section

In situ X-ray photoelectron spectroscopy (XPS) experiments were performed at beamlines U49/2-PGM1 and PGM2 at BESSY, Berlin. Pd 3d core levels of a Pd foil sample were recorded at normal emission with 720 eV excitation, corresponding to an inelastic mean free path of approximately 9 Å.[15]

In situ prompt gamma activation analysis (PGAA) was carried out at the cold neutron beam of the Budapest Neutron Centre, Budapest, Hungary.[16] H/Pd molar ratios of 7 mg Pd black were determined under different conditions from the characteristic peak areas corrected by the detector efficiency and the nuclear data of the detected elements.[8]

The 20 bar acetylene hydrogenation was carried out in a continuous-flow microreactor with on-line GC using a 0.02% Pd/alumina catalyst.

Density functional theory-based calculations on slab models have been carried out to investigate the accumulation of carbon on and in Pd(111). The adsorption energy was evaluated using the PW91 function.[17] The PAW method[18] was used to represent the inner cores and one electron states were expanded in a plane wave basis with a kinetic cut-off energy of 400 eV. A Monkhorst-Pack mesh with 11 × 11 × 1 and 9 × 9 × 1 k-points was used for small and large cells.[19]

For more experimental details, please consult the Supporting Information available online.

[1] a) H. Arnold, F. Dobert, J. Gaube in *Hydrogenation Reaction in Handbook of Heterogeneous Catalysis*, Vol. 5 (Eds.: G. Ertl, H. Knozinger, J. Weitkamp), Wiley–VCH, New York, **1997**, p. 2165; b) A. Molnar, A. Sarkany, M. Varga, *J. Mol. Catal. A* **2001**, *173*, 185.

[2] A. Borodziñski, G. C. Bond, *Catal. Rev.* **2006**, *48*, 91, and references therein.

[3] a) D. Teschner, J. Borsodi, A. Wootsch, Zs. Révay, M. Hävecker, A. Knop-Gericke, S. D. Jackson, R. Schlögl, *Science* **2008**, *320*, 86; b) D. Teschner, E. M. Vass, M. Hävecker, S. Zafeiratos, P. Schnörch, H. Sauer, A. Knop-Gericke, R. Schlögl, M. Chamam, A. Wootsch, A. S. Canning, J. J. Gamman, S. D. Jackson, J. McGregor, L. F. Gladden, *J. Catal.* **2006**, *242*, 16.

[4] A. D. Johnson, S. P. Daley, A. L. Utz, S. T. Ceyer, *Science* **1992**, *257*, 223.

[5] a) A. Michaelides, P. Hu, A. Alavi, *J. Chem. Phys.* **1999**, *111*, 1343; b) V. Ledentu, W. Dong, P. Sautet, *J. Am. Chem. Soc.* **2000**, *122*, 1796.

[6] Thickness of the Pd/C phase was calculated, assuming only inelastic scattering, using the formula : $d = (\text{IMFP}/\cos\grave{E})*(1+I^{335.6\,\text{eV}}/I^{335\,\text{eV}})$, where I is the corresponding peak area, $\grave{E}$ the takeoff angle, and IMFP the inelastic mean free path. IMFP was 9 Å at 720 eV. The growth of the Pd/C phase was determined from the temporal evolution of the thickness.

[7] H. Yokoyama, H. Numakura, M. Koiwa, *Acta mater.* **1998**, *46*, 2823.

[8] *Handbook of Prompt Gamma Activation Analysis with Neutron Beams* (Ed.: G. L. Molnár), Kluwer Academic Publishers, Dordrecht, **2004**.

[9] Zs. Révay, T. Belgya, L. Szentmiklósi, Z. Kis, A. Wootsch, D. Teschner, M. Swoboda, R. Schlögl, J. Borsodi, R. Zepernick, *Anal. Chem.* **2008**, *80*, 6066.

[10] H. Frieske, E. Wicke, *Ber. Bunsen-Ges.* **1973**, *77*, 48.

[11] G. Kresse, J. Hafner, *Phys. Rev. B* **1993**, *47*, 558.

[12] L. Gracia, M. Calatayud, J. Andrés, C. Minot, M. Salmeron, *Phys. Rev. B* **2005**, *71*, 033407.

[13] K. Reuter, M. Scheffler, *Phys. Rev. B* **2003**, *68*, 045407.

[14] a) W. Dong, V. Ledentu, P. Sautet, A. Eichler, J. Hafner, *Surf. Sci.* **1998**, *411*, 123; b) J.-F. Paul, P. Sautet, *Phys. Rev. B* **1996**, *53*, 8015.

[15] S. Tanuma, C. J. Powell, D. R. Penn, *Surf. Interface Anal.* **1991**, *17*, 911.

[16] Zs. Révay, T. Belgya, Zs. Kasztovszky, J. L. Weil, G. L. Molnár, *Nucl. Instrum. Methods Phys. Res. Sect. B* **2004**, *213*, 385.

[17] J. P. Perdew, J. A. Chevary, S. H. Vosko, K. A. Jackson, M. R. Pederson, D. J. Singh, C. Fiolhais, *Phys. Rev. B* **1992**, *46*, 6671.

[18] P. E. Blöchl, *Phys. Rev. B* **1994**, *50*, 17953.

[19] H. J. Monkhorst, J. D. Pack, *Phys. Rev. B* **1976**, *13*, 5188.